International Journal of Thermophysics, Vol. 25, No. 3, May 2004 (© 2004)

Viscosity and Speed of Sound of Gaseous Nitrous Oxide and Nitrogen Trifluoride Measured with a Greenspan Viscometer

J. J. Hurly[1]

Received November 24, 2003

The viscosity and speed of sound of gaseous nitrous oxide and nitrogen trifluoride were measured using a Greenspan acoustic viscometer. The data span the temperature range 225–375 K and extend up to 3.4 MPa. The average relative uncertainty of the viscosity is 0.68% for N_2O and 1.02% for NF_3. The largest relative uncertainties were 3.09 and 1.08%, respectively. These occurred at the highest densities (1702 $mol \cdot m^{-3}$ for N_2O and 2770 $mol \cdot m^{-3}$ for NF_3). The major contributor to these uncertainties was the uncertainty of the thermal conductivity. The speeds of sound measured up to 3.4 MPa are fitted by a virial equation of state that predicts gas densities within the uncertainties of the equations of states available in the literature. Accurate measurements of the speed of sound in both N_2O and NF_3 have been previously reported up to 1.5 MPa. The current measurements agree with these values with maximum relative standard deviations of 0.025% for N_2O and 0.04% for NF_3.

KEY WORDS: equation of state; Greenspan viscometer; nitrogen trifluoride; nitrous oxide; speed of sound; transport properties; viscosity.

1. INTRODUCTION

The viscosity $\eta(T, p)$ of gaseous nitrous oxide (N_2O) and nitrogen trifluoride (NF_3) was determined as a function of temperature and pressure by interpreting the frequency-response data from a Greenspan acoustic viscometer. The speed of sound $u(T, p)$ was also determined, although the

[1] Process Measurements Division, Chemical Science and Technology Laboratory, National Institute of Standards and Technology, Gaithersburg, Maryland 20899-8360, U.S.A. E-mail: john.hurly@nist.gov

0195-928X/04/0500-0625/0

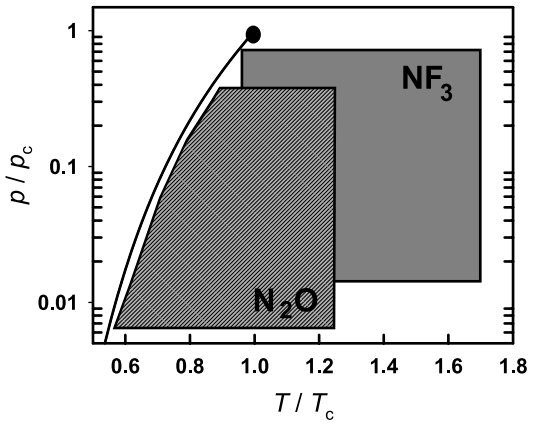

Fig. 1. Reduced pressure and temperature regions spanned by the viscosity measurements. The reduced vapor pressure curve and critical point are also shown.

apparatus was optimized for the measurement of viscosity. The measurements span the temperature range 225–375 K, and pressures up to the lesser of 80% the vapor pressure or 3.4 MPa. Figure 1 shows the reduced temperature and pressure regions of the viscosity measurements for each gas.

The viscosity of N_2O at atmospheric pressure has been measured by several investigators [1–10]. Three investigators measured the density dependence of η at higher pressures. Schlumpf et al. [11] worked at pressures from 10–50 MPa but only reported values graphically; Yokoyama et al. [12] explored mainly the region near the critical point; and Takahashi et al. [13] reported results between 298 and 398 K, and at pressures up to 24 MPa. The present results fill in the density dependence of η below 298 K. A literature search found no previously published measurements of the viscosity of NF_3.

The viscosities were determined by interpreting frequency-response data from a Greenspan acoustic viscometer. In 1953, Greenspan and Wimenitz [14] proposed determining the viscosity of gases by measuring the energy losses in a double Helmholtz acoustic resonator. Subsequently, Gillis et al. [15–17] developed a detailed acoustic model for the Greenspan viscometer that accounts for: (a) viscous boundary losses in the duct, (b) the effects of the convergent–divergent flows at each end of the duct, (c) thermal losses at the gas-resonator boundary, and (d) attenuation of sound throughout the volume of the gas (such as the attenuation caused by either the translation–vibration relaxation or by density fluctuations near the critical point). Hurly et al. [18] gave a detailed account of the

implementation of the model and the apparatus. They calibrated the viscometer with helium and evaluated its performance using five reference gases: Ar, CH_4, C_3H_8, N_2, and SF_6. Hurly et al. [18] also reported $\eta(T, p)$ in gaseous CF_4 and C_2F_6. The reader should refer to the previous publications for details of the acoustic model and the apparatus.

2. NITROUS OXIDE

The critical constants of nitrous oxide are: $T_c = 309.57$ K [19], $p_c = 7.245$ MPa, and the critical volume $V_c = 0.0974$ $m^3 \cdot kmol^{-1}$ [19]. Figure 1 shows the reduced critical point and vapor pressure of N_2O [20] and the experimental temperature and pressure ranges. The molar mass of N_2O is 0.0440128 $kg \cdot mol^{-1}$ [21]. The gas sample was 99.998% N_2O by mass, as indicated by the supplier.

2.1. Results

Table I reports the viscosity of N_2O at 148 pressures and temperatures along seven isotherms between 225 and 375 K. Table I also reports the speed of sound u, a calculated density ρ ($mol \cdot m^{-3}$), and an estimate of the uncertainty of the reported values of η. The densities listed in Table I were calculated using the virial equation of state of Hurly [22]. This equation of state was obtained by fitting speed-of-sound data only up to 1.5 MPa. In this region, the speeds of sound reported in Table I agree with those calculated from the virial equation of state to better than 0.025% as seen in Fig. 2. At pressures greater than 1.5 MPa, the equation of state was extrapolated, and the measured speeds of sound differ by as much as 0.16%. Figure 3 (left) shows the viscosity data along isotherms as a function of pressure. Figure 3 also shows the fit discussed in Section 2.3 and the viscosity estimated using the corresponding states model of Klein et al. [23].

2.2. Uncertainty Analysis

The uncertainty of the tabulated viscosities was determined in the same manner as in Ref. 18. The kinematic viscosity η/ρ was determined by fitting the frequency response of the Greenspan viscometer using the model for the viscometer [Eq. (36) of Ref. 17]. The model requires as inputs: the amplitude (voltage of detector) as a function of the frequency through the resonance, the dimensions of the resonator, temperature, pressure, the molar mass (composition), the heat-capacity C_p, and the thermal conductivity λ. The density ρ, is required if η is to be determined from η/ρ.

Table I. Viscosity (η) and Speed-of-Sound (c) Measurements in N_2O [a]

P (kPa)	ρ (mol · m^{-3})	c (m · s^{-1})	η (μPa · s)	p (kPa)	ρ (mol · m^{-3})	c (m · s^{-1})	η (μPa · s)
			$T = 225$ K				
599.4	350.5	223.98	11.22 ± 0.08	318.3	177.8	230.05	11.15 ± 0.08
561.3	326.1	224.83	11.19 ± 0.08	268.3	148.8	231.07	11.16 ± 0.08
524.6	302.9	225.65	11.18 ± 0.08	208.4	114.6	232.26	11.16 ± 0.08
460.5	263.1	227.06	11.16 ± 0.08	163.6	89.4	233.12	11.17 ± 0.08
405.7	229.7	228.24	11.16 ± 0.08	153.0	83.5	233.32	11.17 ± 0.09
358.7	201.6	229.23	11.16 ± 0.08				
			$T = 250$ K				
1416.1	805.7	224.47	12.56 ± 0.10	640.8	329.1	238.12	12.39 ± 0.09
1335.1	750.6	226.00	12.52 ± 0.10	558.8	284.4	239.41	12.39 ± 0.08
1246.3	691.5	227.70	12.49 ± 0.10	488.8	246.9	240.48	12.38 ± 0.08
1156.7	633.7	229.37	12.46 ± 0.10	428.6	215.1	241.40	12.38 ± 0.08
1073.5	581.4	230.87	12.45 ± 0.09	355.0	176.8	242.49	12.38 ± 0.08
996.0	534.0	232.24	12.44 ± 0.09	296.5	146.8	243.35	12.39 ± 0.08
924.1	490.9	233.48	12.42 ± 0.09	235.8	116.0	244.23	12.37 ± 0.09
857.3	451.6	234.61	12.42 ± 0.09	171.4	83.8	245.15	12.37 ± 0.09
795.4	415.9	235.64	12.41 ± 0.09	111.3	54.1	246.00	12.37 ± 0.11
738.4	383.5	236.57	12.40 ± 0.09	106.6	51.8	246.08	12.38 ± 0.10
			$T = 275$ K				
2904.1	1702.4	219.44	14.33 ± 0.15	1487.6	733.5	240.84	13.78 ± 0.10
2811.8	1625.5	220.97	14.27 ± 0.14	1307.0	633.7	243.17	13.75 ± 0.10
2706.2	1539.7	222.75	14.21 ± 0.14	1149.4	549.5	245.16	13.71 ± 0.10
2578.4	1439.9	224.90	14.15 ± 0.13	1010.5	477.3	246.87	13.69 ± 0.09
2441.4	1338.3	227.12	14.08 ± 0.13	888.5	415.4	248.34	13.67 ± 0.09
2309.7	1245.0	229.17	14.07 ± 0.12	780.6	361.8	249.63	13.66 ± 0.09
2183.6	1159.2	231.07	14.01 ± 0.12	686.0	315.5	250.74	13.65 ± 0.09
2057.0	1076.1	232.95	13.98 ± 0.11	566.5	258.2	252.11	13.64 ± 0.09
1932.5	997.1	234.74	13.91 ± 0.11	468.4	211.9	253.23	13.63 ± 0.09
1812.1	923.0	236.44	13.88 ± 0.11	364.4	163.5	254.40	13.63 ± 0.09
1697.6	854.5	238.02	13.84 ± 0.10	267.9	119.4	255.47	13.62 ± 0.09
1589.4	791.4	239.48	13.81 ± 0.10				
			$T = 300$ K				
3302.7	1657.9	236.86	15.66 ± 0.14	1592.1	700.6	254.48	15.06 ± 0.10
3224.0	1606.9	237.73	15.66 ± 0.13	1405.5	611.1	256.24	15.00 ± 0.10
3125.4	1544.4	238.81	15.61 ± 0.13	1241.1	534.0	257.76	14.97 ± 0.10
3006.7	1470.5	240.11	15.55 ± 0.13	1095.5	467.2	259.10	14.95 ± 0.10
2876.7	1391.5	241.52	15.49 ± 0.12	967.0	409.2	260.27	14.93 ± 0.10
2741.1	1311.3	242.96	15.43 ± 0.12	853.2	358.6	261.29	14.90 ± 0.09
2597.3	1228.3	244.48	15.37 ± 0.12	752.7	314.5	262.19	14.89 ± 0.09
2452.4	1146.9	245.98	15.31 ± 0.11	1183.2	258.9	263.33	14.88 ± 0.09
2310.4	1069.0	247.43	15.27 ± 0.11	1130.3	213.6	264.26	14.87 ± 0.09
2174.1	995.9	248.80	15.22 ± 0.11	404.5	165.7	265.25	14.85 ± 0.09
2044.2	927.7	250.10	15.17 ± 0.11	297.7	121.3	266.17	14.85 ± 0.09

Table I. (*Continued*)

P (kPa)	ρ (mol · m^{-3})	c (m · s^{-1})	η (μPa · s)	p (kPa)	ρ (mol · m^{-3})	c (m · s^{-1})	η (μPa · s)
1921.1	864.4	251.31	15.13 ± 0.11	195.0	79.0	267.05	14.84 ± 0.10
1804.8	805.6	252.44	15.11 ± 0.10	109.2	44.0	267.79	14.83 ± 0.11
1695.3	751.1	253.50	15.07 ± 0.10				
			T = 325 K				
3086.7	1321.6	256.70	16.72 ± 0.12	1357.3	532.7	269.26	16.21 ± 0.10
2896.2	1227.7	258.07	16.65 ± 0.12	1196.2	466.0	270.39	16.18 ± 0.10
2768.2	1165.3	259.02	16.60 ± 0.12	1053.2	407.7	271.40	16.15 ± 0.10
2632.2	1100.1	260.04	16.56 ± 0.11	926.7	356.7	272.28	16.13 ± 0.09
2493.4	1034.5	261.06	16.50 ± 0.11	815.1	312.2	273.06	16.11 ± 0.10
2356.0	970.6	262.07	16.47 ± 0.11	672.2	312.2	274.04	16.10 ± 0.10
2222.6	909.5	263.05	16.43 ± 0.12	554.3	209.9	274.85	16.08 ± 0.10
2093.9	851.3	263.98	16.39 ± 0.11	428.8	161.5	275.71	16.06 ± 0.09
1970.7	796.4	264.87	16.35 ± 0.11	311.6	116.8	276.52	16.06 ± 0.10
1853.7	744.8	265.72	16.32 ± 0.10	200.5	74.8	277.27	16.04 ± 0.11
1742.6	696.5	266.52	16.29 ± 0.11	115.9	43.1	277.85	16.04 ± 0.12
1538.9	609.1	267.97	16.25 ± 0.10				
			T = 350 K				
3251.3	1253.7	270.42	17.92 ± 0.12	1480.8	534.8	280.09	17.42 ± 0.10
3046.3	1165.9	271.48	17.85 ± 0.12	1299.3	466.3	281.09	17.39 ± 0.11
2905.4	1105.9	272.24	17.80 ± 0.12	1139.4	406.7	281.96	17.35 ± 0.10
2756.8	1043.4	273.06	17.75 ± 0.11	998.4	354.6	282.74	17.34 ± 0.10
2605.9	980.6	273.89	17.71 ± 0.11	874.5	309.3	283.42	17.31 ± 0.10
2457.2	919.5	274.71	17.66 ± 0.11	765.8	269.9	284.01	17.30 ± 0.10
2313.1	860.9	275.51	17.63 ± 0.11	627.6	220.1	284.77	17.27 ± 0.10
2174.5	805.2	276.27	17.59 ± 0.11	514.5	179.8	285.39	17.26 ± 0.09
2042.3	752.6	277.00	17.56 ± 0.11	394.8	137.4	286.04	17.25 ± 0.10
1916.8	703.1	277.69	17.52 ± 0.11	284.1	98.5	286.64	17.23 ± 0.10
1797.9	656.7	278.35	17.49 ± 0.10	180.5	62.4	287.21	17.22 ± 0.11
1685.8	613.3	278.96	17.48 ± 0.10	109.4	37.7	287.60	17.20 ± 0.13
1480.8	534.8	280.09	17.42 ± 0.10				
			T = 375 K				
3269.4	1146.2	283.46	19.04 ± 0.12	1351.5	449.2	291.53	18.57 ± 0.11
3049.0	1062.6	284.31	18.97 ± 0.12	1181.1	390.7	292.26	18.52 ± 0.10
2901.3	1006.8	284.93	18.93 ± 0.12	1031.3	339.8	292.91	18.49 ± 0.10
2745.6	948.6	285.58	18.88 ± 0.11	900.3	295.6	293.48	18.47 ± 0.10
2588.9	890.4	286.24	18.84 ± 0.11	733.7	239.9	294.21	18.45 ± 0.10
2435.5	834.0	286.89	18.80 ± 0.12	598.1	194.8	294.80	18.45 ± 0.10
2287.6	780.1	287.51	18.77 ± 0.11	455.4	147.8	295.42	18.42 ± 0.10
2146.1	729.0	288.11	18.73 ± 0.11	323.9	104.8	296.01	18.40 ± 0.11
2011.7	680.8	288.69	18.70 ± 0.11	202.1	65.2	296.54	18.38 ± 0.12
1884.4	635.4	289.23	18.67 ± 0.11	136.2	43.8	296.83	18.40 ± 0.12
1764.1	592.9	289.75	18.63 ± 0.11	110.9	35.7	296.94	18.40 ± 0.14
1544.8	516.1	290.69	18.60 ± 0.11				

[a] Densities calculated with Ref. 38.

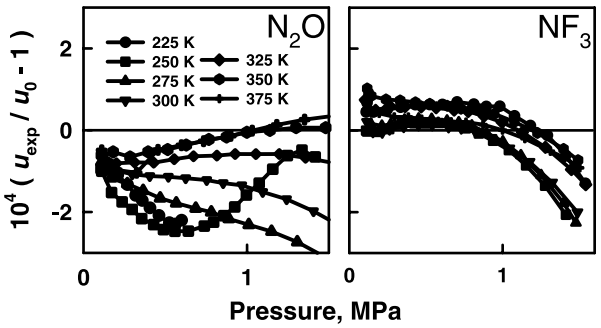

Fig. 2. Relative deviations of the present speed-of-sound data from a fit to previously reported measurements for N_2O [38] and NF_3 [36] up to 1.5 MPa.

At each temperature and pressure, the complex frequency response of the resonator was measured at 22 uniformly spaced frequencies spanning twice the half-width, $\pm 2g$, about the resonance frequency f_0 of the Helmholtz mode. The contribution of the frequency synthesizer to the uncertainties is insignificant. The complex ratio (source voltage)/(detector

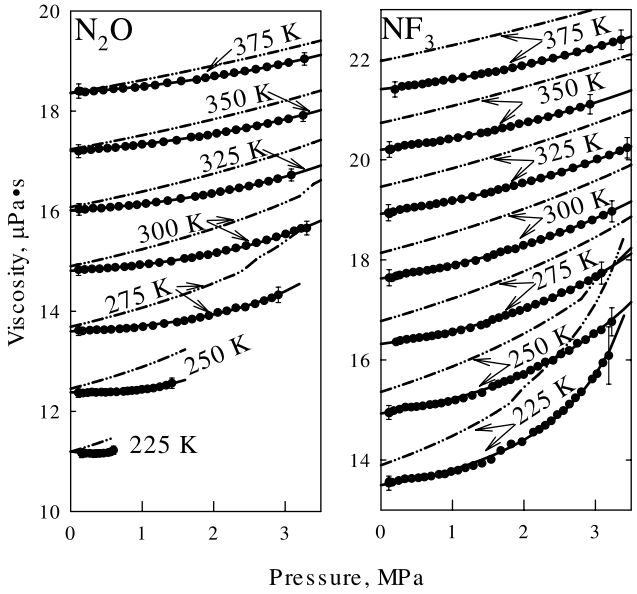

Fig. 3. Present viscosity measurements are shown along each isotherm as a function of pressure. The fit to Eq. (1) is shown as the solid lines through the points. The viscosities estimated using the corresponding states theory of Klien [23] are shown as (– ·· –).

voltage) was measured with two lock-in amplifiers. Each lock-in amplifier measured the real and imaginary voltage components approximately 400 times during 8 s and returned the mean values and their standard deviations. These standard deviations (coverage factor of $k = 2$ always used) were used to weight each point when fitting the model to the frequency response. The frequencies were scanned upward and then downward, resulting in 44 values. Scanning up and down through the resonance provides redundant data that were used to check reproducibility. Averaging the up and down data greatly reduces the effects of small temperature drifts. The redundant data at each frequency and the standard deviation of each voltage propagate through to the standard deviation of the fit to the model, which is included in the summation of uncertainties.

The dimensions of the viscometer were accurately measured with a coordinate measuring machine. The largest source of uncertainty in this category arises from the poorly characterized geometry of the ends of the main duct. This required a calibration of the resonator with helium, and an adjustment of a resistive end-effect parameter [17]. Because we calibrated the viscometer with helium at 298 K, the uncertainties resulting from the dimensional measurements are insignificant for the other gases and at other temperatures.

The estimated uncertainty in the measured temperature with the SPRT is 10 mK. The estimated uncertainty in pressure measurements is typically less than 0.2 kPa. For each gas in the range studied, the viscosity $\eta(T, p)$ depended only weakly on temperature and pressure. Each property was changed within its estimated uncertainty, and the viscosity was re-calculated with the full model to determine how the uncertainty propagated into the reported viscosities.

Reference 22 reports the ideal-gas heat capacity with an uncertainty of $\pm$ 0.1% and an equation of state from which densities are calculated to $\pm$ 0.1%. The equation of state was only fit to pressures up to 1.5 MPa and had to be extrapolated to higher pressures. The speed of sound calculated from this equation of state agrees with the measurements to better than 0.025% relative uncertainty below 1.5 MPa. This is evidence that no significant uncertainty arises from impurities. An additional uncertainty of 0.05% in the density was included at pressures above 1.5 MPa, where the virial equation of state was extrapolated and compared to an independent equation of state [24].

The largest source of uncertainty comes from the uncertainty in the thermal conductivity, λ. The Greenspan viscometer is optimized to maximize viscous losses (80–95%) and minimize thermal losses (5–20%); however, the thermal losses must be subtracted from the total to determine η. The thermal conductivity was taken from the extended corresponding

states model of McLinden et al. [25] and the relative uncertainties estimated to be 4%. Millat et al. [26] reported the only experimental $\lambda(T, p)$ data for N_2O found in the literature. Their results span the temperature range 308–430 K at pressures up to 11 MPa and agree with those predicted by Ref. 25 within 3% relative standard deviation over this range. Millat et al. measurements were estimated to have a relative uncertainty of 3% by comparing their results for argon to those of Sun et al. [27]. However, since we had no data to compare below 308 K the relative uncertainty in λ was estimated as 4%. The thermal conductivity was then changed within its estimated uncertainty, and the viscosity was re-calculated with the full model to determine how the uncertainty propagated into the reported viscosities, and then included in the summed relative uncertainties reported in Table I.

The final category of uncertainty is that from the model used to reduce the data [17]. The viscometer was calibrated using the viscosity of helium [17] as determined by *ab initio* calculations [28], reproducing the helium viscosity to 0.06%. Reference 18 compared the viscosities measured using the model for five reference gases. In all cases, the viscosities agreed within the uncertainties of the reference gases. The standard deviation of the fit of the model to the frequency response of the viscometer is included in the total uncertainty. At each T and p three redundant measurements are made and the average, weighted by the standard deviations of the fit, are reported in Table I. The reported uncertainty for each viscosity is the larger of the summation of the uncertainties listed above or the standard deviation of the three identical measurements. In almost all cases it was the summation of uncertainties which was the larger of the two.

2.3. Analysis

The viscosity virial expansion as a function of density,

$$\eta(T, p) = \eta_0(T)\left[1 + B_\eta(T)\,\rho(T, p) + C_\eta(T)\,\rho^2(T, p)\right] \tag{1}$$

was fit to each isotherm. The resulting values of the zero-density viscosity η_0, B_η, and C_η are listed in Table II. Table II also lists the relative standard deviations of the fits to each isotherm. The zero-density viscosities are fitted by the empirical function of temperature:

$$\eta_0(T)/(\mu Pa \cdot s) = 0.05804(T/\mathrm{K})^{0.9715} \tag{2}$$

with a relative standard deviation of 0.08%. Figure 4 shows the relative deviations from Eq. (2) of this work and of the values of η_0 previously

Table II. Coefficients for Eq. (1)

T (K)	$\eta_0(T)\mu$Pa · s)	$B_\eta(T)$(cm^3 · mol^{-1})	$C_\eta(T)$(cm^3 · kmol^{-1})^2	σ_{fit}(%)
N_2O				
225	11.20	−44.05	125, 626	0.038
250	12.38	−7.78	30, 876	0.035
275	13.60	11.1	12, 232	0.066
300	14.81	14.0	13, 196	0.047
325	16.02	15.0	13, 858	0.019
350	17.20	18.7	11, 886	0.035
375	18.37	16.3	13, 695	0.037
NF_3				
225	13.50	29.8	14, 851	0.200
250	14.93	29.6	15, 961	0.132
275	16.32	25.7	18, 365	0.074
300	17.63	30.3	15, 096	0.057
325	18.92	31.2	13, 084	0.045
350	20.20	26.6	14, 716	0.038
375	21.41	23.9	14, 921	0.025

reported by other investigators. The values of B_η and C_η in Table II were fitted by the empirical functions of temperature resulting in

$$B_\eta(T)/(\text{cm}^3 \cdot \text{mol}^{-1}) = -141.82 + 1.158 \times 10^5 (T/\text{K})^{-1} - 2.09 \times 10^7 (T/\text{K})^{-2} \quad (3)$$

$$C_\eta(T)/(\text{cm}^6 \cdot \text{mol}^{-2}) = (-1.644 \times 10^{-4} + 7.66 \times 10^{-7} (T/\text{K}))^{-1} \quad (4)$$

Equations (2)–(4) used in Eq. (1) allow the calculation of the viscosity in N_2O over the experimental temperature and pressure ranges, 225 to 375 K and pressures up to 3.3 MPa.

Figure 5 shows the values of $B_\eta(T)$ listed in Table II, Eq. (3), and the values obtained by fitting the values of $\eta(T, p)$ from Refs. 12 and 13 to Eq. (1). Figure 4 also shows the predicted values $B_\eta(T)$ using the Rainwater–Friend theory [29] as implemented by Bich and Vogel [30] using the Lennard-Jones parameters given in Ref. 30 ($\varepsilon/k_B = 248.8$, $\sigma = 0.3776$ nm) and also the parameters given by Reid et al. [31] ($\varepsilon/k_B = 232.4$, $\sigma = 0.3828$ nm). A Lennard-Jones potential fit to Eq. (2) using the rigorous kinetic theory of gases [32] results in the values of $\varepsilon/k_B = 241.85$, $\sigma = 0.3799$ nm with a relative standard deviation of 0.5% over the experimental temperature range. These parameters predict $B_\eta(T)$ between the other two sets of parameters.

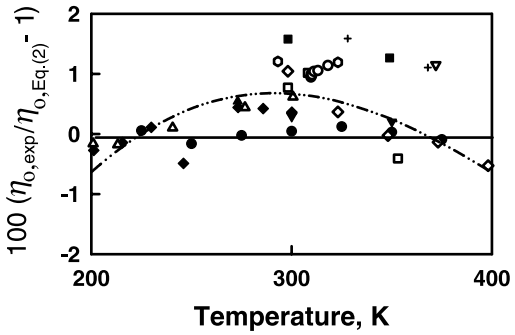

Fig. 4. Percent relative deviations of the zero-density viscosity of N_2O from Eq.(2). Key: (●) present work, (–···–) Ref. 23, (■) Ref. 1, (▲) Ref. 2, (▼) Ref. 3, (⧫) Ref. 4, (□) Ref. 6, (△) Ref. 7, (✚) Ref. 8, (▽) Ref. 9, (⬡) Ref. 10, (○) Ref. 12, (◊) Ref. 13.

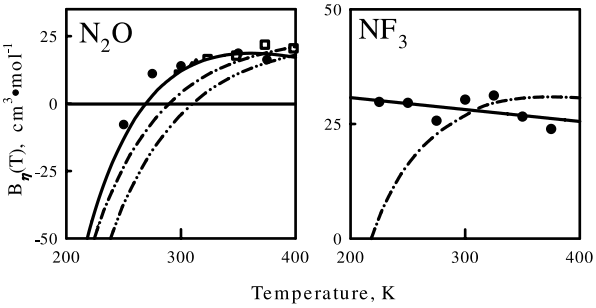

Fig. 5. Second viscosity virial coefficient $B_\eta(T)$ as a function of temperature. Key: (●) present work, (———) Eqs. (3) and (6), (□) Ref. 13, (△) Ref. 12, (– · –) predicted values using Refs. 29 and 30, (— ·· —) predicted values using Refs. 29 and 30 and the Lennard-Jones parameters of Ref. 31.

3. NITROGEN TRIFLUORIDE

The critical constants of nitrogen trifluoride are $T_c = 234.0$ K [33], $p_c = 4.4607$ MPa [34], and $V_c = 0.11875$ m$^3 \cdot$ kmol^{-1} [35]. The vapor pressure is given in Ref. 34. Figure 1 shows the reduced critical point and vapor pressure of NF_3 [34] and the experimental temperature and pressure ranges. The molar mass of nitrogen trifluoride is 0.0710191 kg $\cdot$ mol^{-1} [21]. The gas sample was 99.998% NF_3 by mass as indicated by the supplier.

3.1. Results

Table III reports the viscosity of NF_3 at 207 pressures and temperatures along seven isotherms between 225 and 375 K at pressures up to 3.4 MPa. Figure 2 (right) shows the viscosity data along isotherms as a function of pressure. Figure 2 also shows the fit discussed in Section 3.3 and the viscosity estimated using the corresponding states model of Klein et al. [23]. Table III also lists the speed-of-sound data, the density calculated from an equation of state [36, 37], and an estimate of the uncertainty of the viscosity. The densities at pressures up to 1.5 MPa that are listed in Table III were calculated using the equation of state of Hurly [36]. This equation of state was only fit to data up to 1.5 MPa. Figure 3 shows that in this region the measured speed of sound agrees with that calculated from the equation of state to better than 0.02%. Above 1.5 MPa, the equation of state of Younglove [37] was used to calculate densities.

3.2. Uncertainty Analysis

The uncertainty of η reported in Table III was evaluated in the same manner as in Section 2.2, and Hurly [38] reported values for the ideal-gas heat capacity with an uncertainty of 0.1%. The thermal conductivity was taken from the extended corresponding states model of McLinden et al. [25] for which we estimated the uncertainty to be 5%. Two equations of state were used to determine the density. Hurly [38] gives a virial equation valid up to 1.5 MPa, with a claimed uncertainty of 0.1%. Above 1.5 MPa, the equation of state of Younglove [37] was used, with an estimated uncertainty of 0.3% in density. The measured speeds of sound below 1.5 MPa agree with those from Ref. 38 to better than 0.025% indicating no composition problems or uncertainties associated with the molar mass. As in Section 2.3, an analysis was performed to evaluate how these uncertainties propagated into the reported viscosities, and the results are listed in Table III.

3.3. Analysis

The viscosity data that were acquired along each isotherm were fitted by Eq. (1). The resulting values of the zero-density viscosity η_0 and the second and third viscosity virial coefficients, B_η and C_η, are listed in Table II along with the relative standard deviations of the fits. The zero-density viscosities were fitted by the empirical function of temperature:

$$\eta^0(T)/(\mu\text{Pa} \cdot \text{s}) = \frac{0.6765(T/\text{K})^{0.622}}{1 + 112/(T/\text{K})} \tag{5}$$

Table III. Viscosity (η) and Speed-of-Sound (c) Measurements in NF_3[a]

P (kPa)	ρ (mol·m^{-3})	c (m·s^{-1})	η (μPa·s)	p (kPa)	ρ (mol·m^{-3})	c (m·s^{-1})	η (μPa·s)
			$T = 225$ K				
3186.7	2769.6	134.77	16.09 ± 0.57	1412.1	870.3	164.02	13.93 ± 0.18
3104.1	2626.6	136.67	15.94 ± 0.47	1292.3	785.0	165.47	13.89 ± 0.18
3022.2	2495.2	138.46	15.72 ± 0.61	1180.8	708.0	166.80	13.84 ± 0.16
2955.6	2395.1	139.86	15.62 ± 0.40	1077.4	638.5	168.01	13.79 ± 0.15
2802.7	2186.2	142.82	15.36 ± 0.37	981.9	575.8	169.11	13.77 ± 0.14
2720.5	2082.7	144.31	15.24 ± 0.34	893.7	519.2	170.11	13.72 ± 0.15
2636.5	1982.0	145.80	15.12 ± 0.32	812.6	468.1	171.02	13.71 ± 0.14
2551.6	1884.8	147.26	14.99 ± 0.31	703.3	400.7	172.22	13.68 ± 0.13
2466.5	1792.0	148.66	14.91 ± 0.29	607.8	343.0	173.26	13.66 ± 0.13
2381.7	1703.3	150.02	14.78 ± 0.30	524.4	293.6	174.15	13.64 ± 0.13
2297.4	1618.5	151.34	14.69 ± 0.27	430.1	238.6	175.15	13.63 ± 0.13
2214.2	1537.8	152.60	14.61 ± 0.27	334.8	184.2	176.15	13.62 ± 0.13
2132.1	1460.9	153.82	14.56 ± 0.26	247.5	135.0	177.05	13.59 ± 0.13
1973.0	1318.9	156.10	14.36 ± 0.25	157.1	85.0	177.97	13.55 ± 0.14
1820.9	1190.3	158.20	14.32 ± 0.21	116.0	62.5	178.40	13.57 ± 0.14
1676.5	1074.1	160.13	14.19 ± 0.23	110.1	59.4	178.46	13.54 ± 0.14
1540.2	964.7	162.42	14.01 ± 0.18				
			$T = 250$ K				
3228.4	2023.7	160.42	16.76 ± 0.28	1412.9	747.8	176.99	15.34 ± 0.15
3080.4	1900.4	161.80	16.60 ± 0.27	1277.2	669.1	178.08	15.29 ± 0.15
2975.3	1815.0	162.80	16.52 ± 0.27	1153.4	598.8	179.08	15.24 ± 0.14
2862.6	1726.3	163.84	16.40 ± 0.25	1040.6	535.9	179.98	15.20 ± 0.14
2747.2	1637.6	164.90	16.33 ± 0.25	938.1	479.6	180.79	15.17 ± 0.13
2631.9	1551.5	165.94	16.19 ± 0.24	845.1	429.3	181.52	15.14 ± 0.13
2518.2	1468.4	166.97	16.12 ± 0.24	760.7	384.2	182.19	15.12 ± 0.13
2407.0	1389.2	167.96	15.99 ± 0.23	684.4	343.9	182.78	15.11 ± 0.13
2299.0	1313.9	168.92	15.96 ± 0.23	583.5	291.2	183.56	15.08 ± 0.13
2194.3	1242.4	169.85	15.87 ± 0.21	497.0	246.6	184.23	15.07 ± 0.13
2093.2	1174.7	170.73	15.79 ± 0.20	423.1	209.0	184.80	15.06 ± 0.13
1995.7	1110.7	171.58	15.71 ± 0.20	341.1	167.5	185.44	15.06 ± 0.12
1901.8	1050.1	172.39	15.68 ± 0.20	260.3	127.2	186.05	15.01 ± 0.13
1811.6	992.8	173.17	15.60 ± 0.19	178.4	86.7	186.68	14.99 ± 0.13
1724.9	938.6	173.92	15.57 ± 0.18	116.0	56.2	187.12	14.94 ± 0.14
1641.7	887.4	174.62	15.52 ± 0.18	109.7	53.1	187.17	14.95 ± 0.14
1562.0	839.0	175.30	15.47 ± 0.18				
			$T = 275$ K				
3085.8	1589.4	177.80	17.74 ± 0.22	1478.1	693.6	187.65	16.73 ± 0.15
3003.3	1539.7	178.24	17.66 ± 0.22	1398.6	653.7	188.10	16.69 ± 0.14
2900.8	1478.3	178.82	17.58 ± 0.22	1251.7	580.8	188.93	16.64 ± 0.14
2780.7	1407.2	179.51	17.50 ± 0.21	1120.0	516.3	189.69	16.60 ± 0.14
2651.8	1331.8	180.27	17.40 ± 0.20	1001.6	459.0	190.36	16.56 ± 0.13
2526.7	1259.7	181.01	17.34 ± 0.21	895.3	408.1	190.97	16.52 ± 0.13

Table III. (*Continued*)

P (kPa)	ρ (mol · m^{-3})	c (m · s^{-1})	η (μPa · s)	p (kPa)	ρ (mol · m^{-3})	c (m · s^{-1})	η (μPa · s)
2401.1	1188.5	181.75	17.24 ± 0.20	799.8	363.0	191.52	16.50 ± 0.13
2279.2	1120.4	182.46	17.17 ± 0.19	714.2	322.8	192.02	16.48 ± 0.13
2161.9	1055.8	183.16	17.11 ± 0.19	637.5	287.1	192.46	16.46 ± 0.13
2049.5	994.7	183.83	17.05 ± 0.19	537.4	240.8	193.03	16.45 ± 0.13
1942.2	937.0	184.47	16.99 ± 0.18	452.8	202.1	193.52	16.43 ± 0.13
1839.9	882.7	185.08	16.94 ± 0.18	360.2	160.1	194.05	16.41 ± 0.13
1742.6	831.6	185.67	16.89 ± 0.18	270.5	119.7	194.57	16.39 ± 0.13
1649.9	783.4	186.22	16.84 ± 0.17	212.9	94.0	194.89	16.36 ± 0.13
1561.8	738.1	186.75	16.81 ± 0.17	140.4	61.8	195.31	16.35 ± 0.14
			$T = 300$ K				
3231.6	1461.5	190.05	18.97 ± 0.21	1488.4	628.2	197.54	18.05 ± 0.14
3110.1	1400.2	190.49	18.89 ± 0.21	1323.2	555.2	198.21	17.99 ± 0.14
2954.6	1322.2	191.09	18.80 ± 0.20	1175.9	490.8	198.83	17.94 ± 0.14
2799.7	1245.3	191.70	18.70 ± 0.20	1044.6	434.0	199.38	17.90 ± 0.14
2649.2	1171.5	192.31	18.61 ± 0.20	927.5	383.8	199.87	17.86 ± 0.13
2504.7	1101.4	192.90	18.55 ± 0.19	823.2	339.4	200.32	17.84 ± 0.13
2367.0	1035.2	193.47	18.48 ± 0.19	730.4	300.1	200.71	17.81 ± 0.13
2235.7	972.9	194.02	18.41 ± 0.18	647.8	265.4	201.07	17.79 ± 0.13
2110.9	914.2	194.54	18.34 ± 0.18	540.8	220.8	201.53	17.77 ± 0.13
1992.5	859.0	195.05	18.29 ± 0.18	451.4	183.7	201.91	17.75 ± 0.13
1880.2	807.1	195.53	18.22 ± 0.18	354.7	143.9	202.34	17.73 ± 0.13
1774.0	758.5	195.98	18.20 ± 0.17	262.5	106.2	202.74	17.70 ± 0.14
1673.4	712.7	196.42	18.16 ± 0.17	215.4	87.0	202.95	17.68 ± 0.13
1578.3	669.9	196.83	18.10 ± 0.17	154.2	62.1	203.21	17.64 ± 0.14
1488.4	628.2	197.54	18.05 ± 0.14	115.3	46.4	203.36	17.64 ± 0.16
			$T = 325$ K				
3445.0	1399.1	200.75	20.24 ± 0.20	1448.7	556.4	206.73	19.32 ± 0.14
3340.9	1353.5	200.98	20.18 ± 0.20	1279.1	489.1	207.25	19.26 ± 0.14
3193.3	1288.6	201.36	20.09 ± 0.20	1129.1	430.1	207.70	19.22 ± 0.14
3024.6	1214.9	201.81	20.01 ± 0.20	996.5	378.3	208.12	19.18 ± 0.14
2853.4	1140.8	202.28	19.92 ± 0.19	879.2	332.7	208.48	19.15 ± 0.13
2686.7	1069.2	202.75	19.84 ± 0.19	775.5	292.7	208.81	19.12 ± 0.13
2528.1	1001.7	203.21	19.75 ± 0.19	684.0	257.6	209.10	19.09 ± 0.13
2378.5	938.6	203.65	19.69 ± 0.19	566.4	212.7	209.48	19.07 ± 0.13
2236.9	879.3	204.07	19.63 ± 0.18	469.0	175.6	209.80	19.05 ± 0.13
2102.8	823.5	204.47	19.58 ± 0.18	364.7	136.2	210.14	19.03 ± 0.13
1976.5	771.4	204.86	19.54 ± 0.18	266.4	99.3	210.46	19.01 ± 0.13
1857.9	722.7	205.23	19.48 ± 0.18	172.0	63.9	210.78	18.96 ± 0.14
1746.1	677.2	205.58	19.44 ± 0.18	118.7	44.1	210.96	18.92 ± 0.16
1640.9	634.6	205.91	19.40 ± 0.17	111.2	41.3	210.99	18.93 ± 0.17
1541.9	593.6	206.46	19.35 ± 0.14	104.3	38.7	211.01	18.94 ± 0.16

Table III. (*Continued*)

P (kPa)	ρ (mol · m^{-3})	c (m · s^{-1})	η (μPa · s)	p (kPa)	ρ (mol · m^{-3})	c (m · s^{-1})	η (μPa · s)
			$T = 350$ K				
2925.3	1065.5	211.94	21.11 ± 0.19	1227.5	431.8	215.67	20.48 ± 0.14
2789.2	1013.3	212.19	21.05 ± 0.19	1077.8	378.0	216.01	20.44 ± 0.14
2639.3	956.0	212.48	20.99 ± 0.19	946.1	331.0	216.31	20.41 ± 0.14
2487.3	898.3	212.79	20.92 ± 0.18	830.2	289.8	216.58	20.38 ± 0.14
2338.7	842.1	213.10	20.86 ± 0.18	728.5	253.8	216.82	20.35 ± 0.13
2196.3	788.6	213.40	20.80 ± 0.18	639.1	222.3	217.03	20.34 ± 0.14
2060.7	737.9	213.69	20.76 ± 0.18	525.2	182.3	217.30	20.32 ± 0.13
1932.7	690.3	213.97	20.72 ± 0.18	431.5	149.5	217.53	20.30 ± 0.14
1812.0	645.6	214.24	20.66 ± 0.18	332.3	114.9	217.78	20.29 ± 0.14
1698.4	603.8	214.50	20.63 ± 0.17	239.8	82.8	218.01	20.25 ± 0.14
1591.7	564.7	214.74	20.59 ± 0.17	143.0	49.3	218.25	20.21 ± 0.15
1491.8	527.4	215.10	20.55 ± 0.14	125.2	43.1	218.30	2 ± 0.20 ± 0.16
1397.8	493.3	215.30	20.53 ± 0.14	117.2	40.3	218.33	20.21 ± 0.16
			$T = 375$ K				
3359.7	1132.1	220.46	22.40 ± 0.20	1503.1	492.4	223.10	21.74 ± 0.14
3247.3	1092.4	220.60	22.35 ± 0.20	1404.4	459.5	223.25	21.72 ± 0.14
3090.6	1037.4	220.78	22.28 ± 0.19	1312.2	428.7	223.39	21.69 ± 0.14
2918.0	977.1	220.99	22.22 ± 0.19	1145.5	373.4	223.64	21.65 ± 0.14
2742.5	916.0	221.22	22.15 ± 0.19	999.9	325.3	223.88	21.62 ± 0.14
2571.3	856.7	221.45	22.09 ± 0.19	872.8	283.4	224.09	21.59 ± 0.14
2407.5	800.2	221.67	22.03 ± 0.19	761.6	246.9	224.28	21.56 ± 0.13
2252.4	747.0	221.90	21.98 ± 0.18	664.5	215.1	224.45	21.54 ± 0.14
2106.5	697.1	222.11	21.93 ± 0.18	579.8	187.5	224.59	21.51 ± 0.14
1969.7	650.6	222.32	21.88 ± 0.18	472.5	152.6	224.78	21.50 ± 0.14
1841.4	607.0	222.52	21.84 ± 0.18	385.1	124.2	224.94	21.48 ± 0.14
1721.1	566.4	222.71	21.79 ± 0.18	293.5	94.5	225.10	21.47 ± 0.14
1608.5	528.4	222.89	21.76 ± 0.18	195.7	62.9	225.28	21.41 ± 0.15

[a] Densities calculated with Ref. 36 for $p < 1.5$ MPa and Ref. 37 for $p > 1.5$ MPa.

with a relative standard deviation of 0.09%. The values of B_η and C_η in Table II were fitted by linear functions of temperature resulting in

$$B_\eta(T)/(\mathrm{cm}^3 \cdot \mathrm{mol}^{-1}) = 35.96 - 0.025(T/\mathrm{K}) \quad (6)$$

$$C_\eta(T)/(\mathrm{cm}^6 \cdot \mathrm{mol}^{-2}) = 18,525 - 10.8(T/\mathrm{K}) \quad (7)$$

Equations (5)–(7) used in Eq. (1) allow the calculation of the viscosity of NF_3 over the experimental temperature and pressure ranges, 225–375 K, and pressures up to 3.4 MPa.

Figure 5 shows the values of $B_\eta(T)$ in Table II and the function Eq. (6) that was fitted to them. No previously published values were

found. Figure 5 also shows the values $B_\eta(T)$ predicted by the Rainwater–Friend theory [29] as implemented by Bich and Vogel [30] using the Lennard-Jones parameters given in Ref. 39 ($\varepsilon/k_B = 175.0$ K, $\sigma = 0.4154$ nm). The predicted values fall below the experimental values at the lower temperatures. If we use Eq. (5) to fit Lennard-Jones potential parameters using the kinetic theory of gases [32], we obtain the values of $\varepsilon/k_B = 173.86$ K, $\sigma = 0.4283$ nm, which can be used to predict $B_\eta(T)$ values just slightly larger than those shown in Fig. 5. These potential parameters reproduce $\eta_0(T)$ calculated from Eq. (2) to better than 0.2% relative standard deviation over the experimental temperature range.

4. SPEED OF SOUND

Tables I and II include values of the speed of sound in N_2O and NF_3 determined from the Greenspan viscometer at the same time that we determined the viscosity. Reference 18 demonstrated that the speeds of sound determined in this way up to 3.2 MPa for five reference gases were within 0.04% of the reference values. Here we expect similar uncertainties. Gillis and Moldover [40] have shown that the density $\rho(T, p)$ calculated from a hard-core square-well virial equation of state fit to a speed-of-sound surface under 1.5 MPa have estimated uncertainties of less than $0.001 \times \rho$. References 36 and 38 report accurate measurements of the speed of sound in gaseous N_2O and NF_3 up to 1.5 MPa and report such equations of state. Figure 3 showed that the sound speeds agree with these previously reported up to 1.5 MPa.

In future work, the Greenspan viscometer will be used to measure the kinematic viscosity for gases where no equation of state is available. In those cases, the speed of sound measurements determined from the viscometer could be used to fit an equation of state to calculate the required densities needed to determine η from η/ρ. Because there are equations of state for NF_3 and N_2O, we tested the approach of Gillis and Moldover [40] at lower reduced temperatures and higher densities. For each gas we used the values of $B(T)$ and $C(T)$ that were determined from the speed-of-sound data in Refs. 36 and 38. A fourth virial coefficient $D(T)$ was then fitted to the speed-of-sound surfaces reported in Tables I and III. For N_2O; $D(T)/(\mathrm{cm}^9 \cdot \mathrm{mol}^{-3}) = 6.818 \times 10^{-13} - 3.066 \times 10^{-10}/(T/\mathrm{K})$ and for NF_3; $D(T)/(\mathrm{cm}^9 \cdot \mathrm{mol}^{-3}) = -6.088 \times 10^{-13} + 2.664 \times 10^{-10}/(T/\mathrm{K})$. The densities for N_2O and NF_3 calculated from the two resulting equations of state were compared to that of Lemmon and Span [24] for N_2O and Younglove [37] for NF_3. Lemmon and Span estimate the uncertainty in density to be between 0.2 and 1.0% at higher temperatures. The equation-of-state fit to the speeds of sound differ with a relative standard

deviation of only 0.05% over the range of our measurements, with a maximum of 0.5% at the lower temperatures approaching the vapor pressure curve. Younglove estimates the uncertainty in density to be 0.3% for NF_3, the densities predicted by the equation of state fit to the speed-of-sound surface differs with a relative standard deviation of 0.18% over the range of our measurements, with a maximum of 0.4% at the lower temperatures where the pressure approaches the vapor pressure curve. The equation-of-state fit to the speed-of-sound surfaces for each species predict gas densities within the uncertainties of the equations of states available in the literature. This agreement supports the premise that the Greenspan viscometer is capable of predicting gas densities with reasonable accuracy via speed-of-sound measurements.

ACKNOWLEDGMENT

This work was funded in part by the National Semiconductor Metrology Program.

REFERENCES

1. W. J. Fisher, *Phys. Rev.* **28**:73 (1909).
2. H. Vogel, *Ann. Phys.* **43**:1235 (1914).
3. M. Trautz and F. Kurz, *Ann. Phys.* **9**:981 (1931).
4. H. L. Johnston and K. E. McClosky, *J. Phys. Chem.* **44**:1038 (1940).
5. C. J. G. Raw and C. P. Ellis, *J. Chem. Phys.* **28**:1198 (1958).
6. P. K. Chakraborti and P. Gray, *Trans. Faraday Soc.* **61**:2422 (1965).
7. E. J. Harris, G. C. Hope, D. W. Gough, and E. B. Smith, *J. Chem. Soc. Faraday Trans. 1* **75**:892 (1979).
8. J. Kestin and W. A. Wakeham, *Ber. Bunsen-Ges. Phys. Chem.* **83**:573 (1979).
9. A. A. Clifford, P. Gray, and A. C. Scott, *J. Chem. Soc. Faraday Trans. 1* **77**:997 (1981).
10. J. Kestin and S. T. Ro, *Ber. Bunsen-Ges. Phys. Chem.* **86**:948 (1982).
11. J. P. Schlumpf, F. Lazarre, and P. Valillet, *J. Chim. Phys.* **72**:631 (1975).
12. C. Yokoyama, M. Takahaashi, and S. Takahasi, *Int. J. Thermophys.* **15**:603 (1994).
13. M. Takahashi, N. Shibasaki-Kitakawa, C. Yokoyama, and S. Takahashi, *J. Chem. Eng. Data* **41**:1495 (1996).
14. M. Greenspan and F. N. Wimenitz, *An Acoustic Viscometer for Gases-I*, NBS Report 2658 (1953).
15. K. A. Gillis, J. B. Mehl, and M. R. Moldover, *Rev. Sci. Instrum.* **67**:1850 (1996).
16. J. Wilhelm, K. A. Gillis, J. B. Mehl, and M. R. Moldover, *Int. J. Thermophys.* **21**:983 (2000).
17. K. A. Gillis, J. B. Mehl, and M. R. Moldover, *J. Acous. Soc. Am*. **114**:166 (2003).
18. J. J. Hurly, K. A. Gillis, J. B. Mehl, and M. R. Moldover, *Int. J. Thermophys.* **24**:1441 (2003).
19. J. F. Mathews, *Chem. Rev.* **72**:71 (1972).
20. K. A. Kobe, L. J. Hirth, and E. J. Couch, *J. Chem. Eng. Data* **6**:229 (1961).

21. IUPAC, *J. Phys. Chem. Ref. Data* **30**:701 (2001).
22. J. J. Hurly, *Int. J. Thermophys.* **21**:805 (2000).
23. S. A. Klein, M. O. McLinden, and A. Laesecke, *Int. J. Refrig.* **20**:208 (1997).
24. E. W. Lemmon and R. Span, preliminary equation (2001); E. W. Lemmon, M. O. McLinden, and M. L. Huber, *NIST Standard Reference Database 23*: *Reference Fluid Thermodynamic and Transport Properties*, *Version 7.0* (National Institute for Standards and Technology, Standard Reference Data Program, Gaithersburg, Maryland, 2002).
25. M. O. McLinden, S. A. Klein, and R. A. Perkins, *Int. J. Refrig.* **23**:43 (2000).
26. J. Millat, M. Mustafa, M. Ross, W. A. Wakeham, and M. Zalaf, *Physica A* **145A**:461 (1987).
27. L. Sun, J. E. S. Venart, and R. C. Prasad, *Int. J. Thermophys.* **23**:357 (2002).
28. J. J. Hurly and M. R. Moldover, *J. Res. Natl. Inst. Stand. Technol.* **105**:667 (2000).
29. J. C. Rainwater and D. G. Freind, *Phys. Rev. A* **36A**:4062 (1987).
30. E. Bich and E. Vogel, *Int. J. Thermophys.* **12**:27 (1991); E. Bich and E. Vogel, in *Transport Properties of Fluids, Their Correlation, Prediction and Estimation*, J. Millat, J. H. Dymond, and C. A. Nieto de Castro, eds. (Cambridge, New York, 1996).
31. R. C. Reid, J. M. Prausnitz, and B. E. Poling, *The Properties of Gases and Liquids*, 4th Ed. (McGraw-Hill, New York, 1987).
32. J. O. Hirschfelder, C. F. Curtiss, and R. B. Bird, *Molecular Theory of Gases and Liquids* (John Wiley, New York, 1954).
33. L. A. Weber, *J. Chem. Thermodyn.* **13**:389 (1981).
34. B. A. Younglove, *J. Phys. Chem. Ref. Data*. *Suppl. 1* **11**:1 (1982).
35. *Nitrogen Trifluoride*, *Speciality Gas Data Sheet* (Air Products, Allentown, Pennsylvania, 1983).
36. J. J. Hurly, *Int. J. Thermophys.* **23**:667 (2002).
37. B. A. Younglove, *J. Phys. Chem. Ref. Data*. *Suppl. 1* **11**:1 (1982).
38. J. J. Hurly, *Int. J. Thermophys.* **24**:1611 (2003).
39. R. A. Svehla, *Estimated Viscosities and Thermal Conductivities of Gases at High Temperatures*, NASA Tech. Rept., NASA TR-132 (1962).
40. K. A. Gillis and M. R. Moldover, *Int. J. Thermophys.* **17**:1305 (1996).